

Catching an Entatic State—A Pair of Copper Complexes**

Alexander Hoffmann, Stephan Binder, Anton Jesser, Roxana Haase, Ulrich Flörke, Manuel Gnida, Marco Salomone Stagni, Wolfram Meyer-Klaucke, Benjamin Lebsanft, Lara Elena Grünig, Simon Schneider, Maryam Hashemi, Arne Goos, Alina Wetzel, Michael Rübhausen, and Sonja Herres-Pawlis*

Dedicated to Professor Bernt Krebs on the occasion of his 75th birthday

Abstract: The structures of two types of guanidine–quinoline copper complexes have been investigated by single-crystal X-ray crystallography, K-edge X-ray absorption spectroscopy (XAS), resonance Raman and UV/Vis spectroscopy, cyclic voltammetry, and density functional theory (DFT). Independent of the oxidation state, the two structures, which are virtually identical for solids and complexes in solution, resemble each other strongly and are connected by a reversible electron transfer at 0.33 V. By resonant excitation of the two entatic copper complexes, the transition state of the electron transfer is accessible through vibrational modes, which are coupled to metal–ligand charge transfer (MLCT) and ligand–metal charge transfer (LMCT) states.

Copper is one of the most important redox-active metals and plays a central role in many biological processes.^[1] Blue copper electron-transfer proteins are nature's workhorses for electron transfer (ET). They use copper as a one-electron relay that shuttles between the cuprous and cupric oxidation states. Their Cu^{II/I} reduction potentials span a large window ($E^\circ = 0.18$ to >1 V versus NHE (normal hydrogen electrode)),^[2] which tailors these proteins to interact with a wide variety of ET partners. The inner coordination sphere most directly affects the redox properties of metal ions.^[3] Hence, tuning the Cu^{II/I} redox couple is central for electron transfer in nature and also important in synthetic complexes for catalytic applications.^[4–6] There are multiple factors governing the redox potential, including the effects of the first coordination

sphere such as geometric constraints enforced by the ligand sphere (tetrahedral versus square-planar coordination) and ligand donor atoms (σ - and/or π -donation), as well as second-coordination-sphere effects.^[7–11]

Already in 1968, Vallee and Williams coined the term “entatic state” (also called rack-induced state), defined as a “catalytically poised state intrinsic to the active site”.^[12] This term has been intensively discussed during the last decades.^[7,13–15] Rorabacher et al. specified it to be an electronic entatic state rather than a simple geometric constraint physically imposed upon the active site by the protein matrix.^[16] Hodgson et al. proved with X-ray absorption spectroscopy (XAS) methods that the concept of a rack-induced state might be not valid as the protein imposes almost no strain on the copper coordination.^[17] Theoretically, it was proven that Cu^{II} prefers square-planar and square-pyramidal coordination but that π -donor ligands lead to stabilization of trigonal distorted geometries.^[18] Recently, Vila et al. found that the entatic state does not require the ligand to have a preformed metal-binding site. They identified metal binding as a major contributor to the conformational rigidity of copper centers involved in electron transfer which reconciles the seemingly contradictory requirements of a rigid center for electron transfer and an accessible, dynamic site for in vivo copper uptake.^[19] In blue copper centers, the entatic state is currently regarded as a “soft entatic state”,^[20] whereas the whole concept has been condensed into an “energization due to a misfit between ligands and metal ions.”^[21]


[*] Dr. A. Hoffmann, A. Jesser, Prof. Dr. S. Herres-Pawlis
Ludwig-Maximilians-Universität München
Department Chemie
81377 München (Germany)
E-mail: sonja.herres-pawlis@cup.uni-muenchen.de

Dr. S. Binder, B. Lebsanft, L. E. Grünig, S. Schneider, M. Hashemi,
A. Goos, A. Wetzel, Prof. Dr. M. Rübhausen
Institut für Angewandte Physik and Center for Free-Electron Laser
Science, Universität Hamburg
22607 Hamburg (Germany)

Dr. R. Haase, Dr. U. Flörke, Dr. M. Gnida, Dr. W. Meyer-Klaucke
Universität Paderborn, Department Chemie
Warburger Strasse 100, 33098 Paderborn (Germany)

Dr. M. Salomone Stagni
Libera Università di Bozen-Bolzano
Faculty of Science and Technology
piazza Università, 1, 39100 Bozen, Bolzano (Italy)

[**] We thank the Deutsche Forschungsgemeinschaft (DFG FOR 1405), the Fonds der Chemischen Industrie (FCI for S.H.-P.), the Evonik-Stiftung (R.H.), and the Bundesministerium für Bildung und Forschung (BMBF 05K12GU1 for A.W. and MoSGrid initiative 01IG09006) for financial support, the beamline staff at the Deutsches Elektronen-Synchrotron (DESY Photon Science (Germany)) and the Diamond Light Source (UK) for assistance with XAS data collection, P. Höfer at the MPI Mülheim for square-wave voltammetric measurements, and the Paderborn Cluster for Parallel Computing (PC² Paderborn) and the Center for Information Services and High Performance Computing of the Technische Universität Dresden for calculation time.

 Supporting information for this article (including details on materials and methods, synthetic procedures, Raman measurements, XAS spectroscopy, cyclic voltammetry, square-wave voltammetry, and DFT details on Raman assignment and excited-state calculations) is available on the WWW under <http://dx.doi.org/10.1002/anie.201306061>.

Here, we report a series of bis(chelate) Cu^I and Cu^{II} complexes in which the cationic units have very similar structures even though Cu^I and Cu^{II} complexes generally prefer tetrahedral and square-planar environments, respectively. Besides the structural study of single crystals in the solid state, we provide insights into the structure in the liquid phase that we obtained from XAS data of complexes in solution. A resonance Raman study of Cu^I and Cu^{II} complexes in solution indicates that both complex types come into resonance at a similar energy around 3.2–3.4 eV. We found a vibrational mode that couples vibronically the optical charge-transfer excitation with the distortion along the reaction coordinate, leading from the Cu^I to the Cu^{II} geometry. Therefore, we have optical access to a charge-separated state which mimics the transition state of the inner-sphere ET. In contrast to reported outer-sphere electron-transfer studies on Cu^{II/I} pairs,^[22] we focus on the photochemically induced charge transfer.

The reaction of tetramethylguanidinoquinoline (TMGqu)^[23] with suitable copper sources yields the series of bis(chelate) Cu^I and Cu^{II} complexes **1–5**. The most remarkable feature of these complexes is their structural similarity (Figure 1, Table 1, and Figures S1–S5 in the Supporting Information). For a Cu^I complex, one would generally expect a structure with tetrahedral configuration as found in [Cu(tmeda)₂]⁺ complexes (tmeda = tetramethylethylenediamine),^[24] whereas Cu^{II} complexes are square-planar (e.g. [Cu(tmeda)₂]²⁺).^[25] But in the complexes **1–5**, the situation is completely different. The copper centers of all complexes are tetracoordinate through interactions with two chelating guanidine–quinoline ligands. The Cu–N_{gua} distances in the Cu^I complexes **1–3** are 0.1 Å longer than those in Cu^{II} complexes **4** and **5**. The contraction of the Cu–N_{qu} bonds during the formal oxidation is not very pronounced (0.02 Å).

The coordination geometry can be described by a τ factor indicating a square-planar arrangement for a value of 0 and an ideal tetrahedron for a value of 1.^[26] In the Cu^I complexes, we

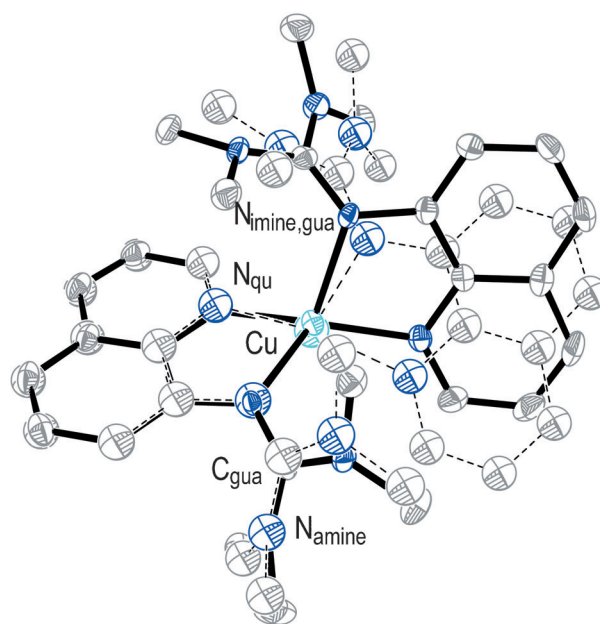


Figure 1. Superimposed molecular structures of [Cu(TMGu)₂]⁺ and [Cu(TMGu)₂]²⁺ (Cu^I: darker with solid bonds, Cu^{II}: lighter with dashed bonds).

observe a τ of roughly 0.6 indicative of a strongly distorted tetrahedron, whereas in the Cu^{II} complexes τ amounts to 0.4. The angle between the chelate planes Cu–N_{gua}–N_{qu} gives a measure of the tetrahedral character as well: 90° correspond to an ideal tetrahedron and 0° to square-planar coordination. This angle ranges from 65.1 to 68.3° in the Cu^I complexes and from 42.5 to 44.6° in the Cu^{II} complexes. This clearly demonstrates that the difference between the two oxidation states results in a twist of approximately 20° between the chelate planes and a shortening of the Cu–N_{gua} bond by 0.1 Å. The guanidine substituents force the ligands to avoid each

Table 1: Key geometric parameters of complexes **1–5**.

| | [Cu(TMGu) ₂](CF ₃ SO ₃) 1 | [Cu(TMGu) ₂](PF ₆) 2 | [Cu(TMGu) ₂](ClO ₄) 3 | [Cu(TMGu) ₂](CF ₃ SO ₃) ₂ 4 | [Cu(TMGu) ₂](PF ₆) ₂ 5 |
|--|--|--|---|---|---|
| Bond lengths [Å] | | | | | |
| Cu–N _{imine,gua} | 2.065(2), 2.113(3) | 2.068(3), 2.095(3) | 2.074(3), 2.080(3) | 1.959(2), 1.964(2) | 1.964(3), 1.964(3) |
| Cu–N _{qu} | 1.978(3), 2.003(2) | 1.966(3), 1.999(3) | 1.998(3), 2.002(3) | 1.976(2), 1.975(2) | 1.967(3), 1.980(3) |
| C _{gua} –N _{imine,gua} | 1.324(4), 1.321(4) | 1.316(4), 1.330(4) | 1.319(4), 1.312(4) | 1.344(3), 1.347(3) | 1.358(4), 1.347(4) |
| C _{gua} –N _{amine,gua} | 1.356(4), 1.359(4) | 1.365(5), 1.357(5) | 1.362(4), 1.352(4) | 1.346(3), 1.343(3) | 1.324(4), 1.346(4) |
| | 1.356(4), 1.372(4) | 1.363(5), 1.355(5) | 1.361(4), 1.359(4) | 1.340(3), 1.341(3) | 1.344(4), 1.344(4) |
| Bond angle [°] | | | | | |
| N–Cu–N | 82.1(1), 81.7(1) | 82.6(1), 82.1(1) | 82.2(1), 81.8(1) | 83.5(1), 83.7(1) | 83.6(1), 83.7(1) |
| Structure factors | | | | | |
| $\tau_4^{[a]}$ | 0.60 | 0.58 | 0.60 | 0.40 | 0.41 |
| $\rho^{[b]}$ | 0.97, 0.96 | 0.96, 0.97 | 0.96, 0.97 | 1.00, 0.99 | 1.02, 1.00 |
| Torsion angles [°] | | | | | |
| $\angle(\text{C}_{\text{gua}}\text{N}_3, \text{CuN}_2)$ | 49.5, 58.6 | 49.1, 58.5 | 53.0, 59.2 | 47.5, 52.1 | 46.9, 47.2 |
| $\angle(\text{N}_{\text{amine}}\text{C}_3, \text{C}_{\text{gua}}\text{N}_3)$ | 30.0(av), 29.9(av) | 30.1(av), 27.7(av) | 30.0(av), 29.0(av) | 28.3(av), 31.1(av) | 30.0(av), 28.5(av) |
| $\angle(\text{CuN}_2, \text{CuN}_2')$ | 68.0 | 65.1 | 68.3 | 42.5 | 44.6 |

[a] $\tau_4 = \frac{360^\circ - (\alpha + \beta)}{141}$.^[26] [b] $\rho = 2a/(b+c)$ with $a = d(\text{C}_{\text{gua}}=\text{N}_{\text{imine,gua}})$, b , and $c = d(\text{C}_{\text{gua}}-\text{N}_{\text{amine}})$.^[27]

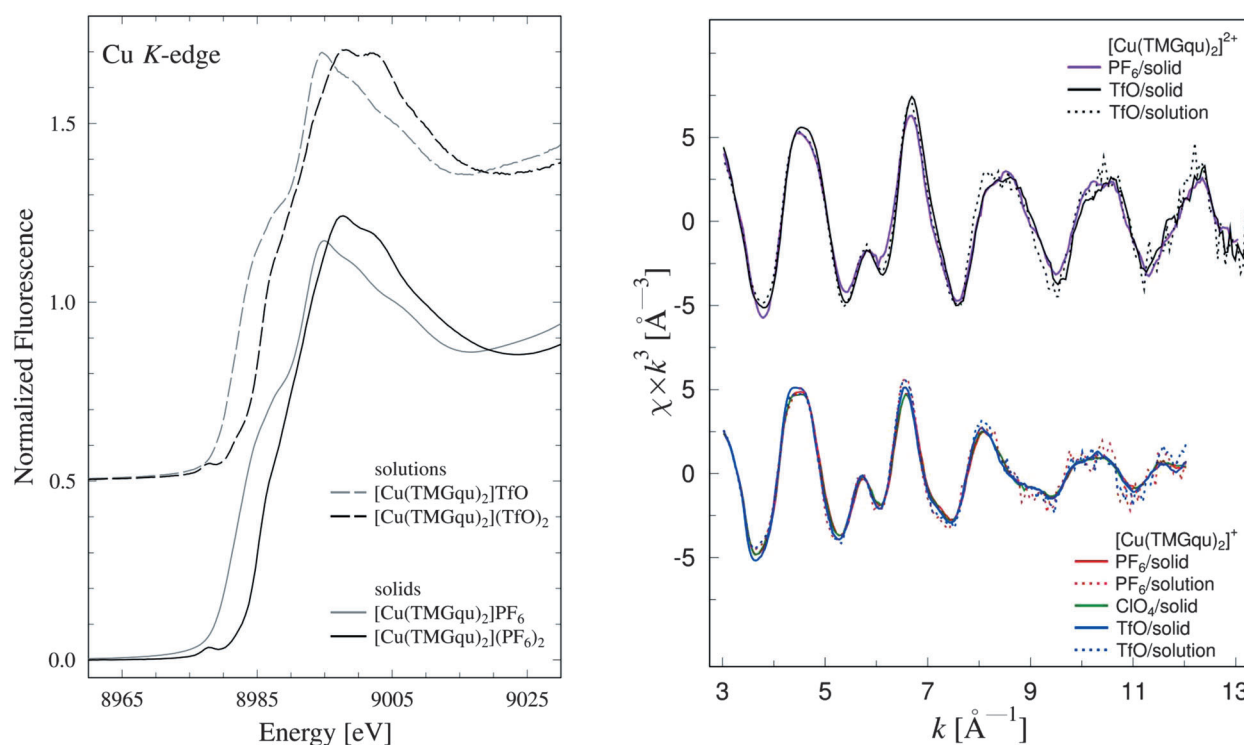


Figure 2. Left: Cu K-edge absorption of solid **2** and **5** (solid curves) as well as solutions of **1** and **4** in MeCN (broken curves). Right: Superimposed experimental k^3 -weighted EXAFS spectra of various Cu^I and Cu^{II} complexes.

other and sterically restrain the coordination geometry to only small variations, ranging from 68 to 44° between the CuN₂ planes and the corresponding range of the τ value from 0.6 to 0.4.

Since the structural change between Cu^I and Cu^{II} is so small, we expected a reversible redox behavior. Cyclic voltammetry proves a reversible oxidation wave for **2** at 0.33 V vs. NHE (Figure S20, left) and square-wave voltammetry shows the 0.33 V oxidation to be a one-electron oxidation step (Figure S20, right).

To characterize the oxidation states we performed XAS spectroscopy on solid samples of **1–5** (see the Supporting Information for details). The solid curves in Figure 3 compare the Cu-K absorption edges of the complexes [Cu(TMGqu)₂](PF₆)₂ (**2**) and [Cu(TMGqu)₂](PF₆)₂ (**5**). The edge positions are 8983.3 eV (**2**) and 8986.8 eV (**5**), equal to a chemical shift between the two compounds of $|\Delta E| = 3.5$ eV. The edge positions and the chemical shift identify the oxidation states as Cu^I in **1–3** and Cu^{II} in **4** and **5** (Figure S6, Table S1).^[28] The oxidation state assignment is further supported by the edge shapes. Cu^I complexes have a characteristic shoulder or peak in the rising edge (8985 eV and below, assigned as a 1s→4p transition).^[28] In contrast, Cu^{II} edges are of rather low intensity in this energy range. The intensity of the “Cu^I feature” can be related to the site geometry. The normalized fluorescence for **2** at 8985.6 eV is 0.65 (Figure 2), indicative of tetracoordinate Cu^I.^[28] The Cu^{II} state in **5**, in turn, manifests itself in a very weak pre-edge peak at 8977.7 eV (Figure 2, left), assignable as a 1s→3d transition.^[29] It is apparent that the edge positions, shapes, and features for Cu^I and Cu^{II} are the same for solid and solution

samples (Figure 2). Analysis of extended X-ray absorption fine structure data (EXAFS) (Table S2, Figure 2, right) demonstrates that, for a given oxidation state, the structural models for solid and solution samples are identical within the precision of the analysis and do not depend on the choice of counterion. Raman data support the conclusion that the structure in solution is independent of the counterion (vide infra and Figure S9). EXAFS analysis of the complexes **2** and **5** confirms the molecular structures as being tetracoordinate with two nitrogen back-scatterers at 2.01 Å and two at 2.03 Å in Cu^I as well as two nitrogen back-scatterers at 1.95 Å and two at 2.00 Å in Cu^{II} (Table S2).

Furthermore, we performed Raman measurements on the complexes **1**, **2**, **4**, and **5** in MeCN and CH₂Cl₂ solution (Figure 3). UV/Vis measurements (see Figures S10–S17) indicated that a resonance can be expected at approximately 3.4 eV and above 4.0 eV for complexes in either oxidation states. The Raman spectra show a multitude of peaks between 400 and 850 cm⁻¹. By exciting at numerous incident photon energies, we derive the excitation dependence of the Raman peak intensities. A vibrational assignment is made possible by theoretical calculations based on extensive benchmarking.^[30] Figure 4a details the excellent agreement between experimental Raman spectra taken with a nonresonant incident photon energy of 2.97 eV and calculated Raman spectra. It is noteworthy that for complex **1** 2.97 eV is clearly in off-resonance condition as the sharp resonance is close to 3.4 eV. Figure 4b compares the experimental Raman data for **4** in nearly nonresonant measurement conditions. The Raman resonance energy is shifted by about 0.3 eV (cf. Figure 3c,d),

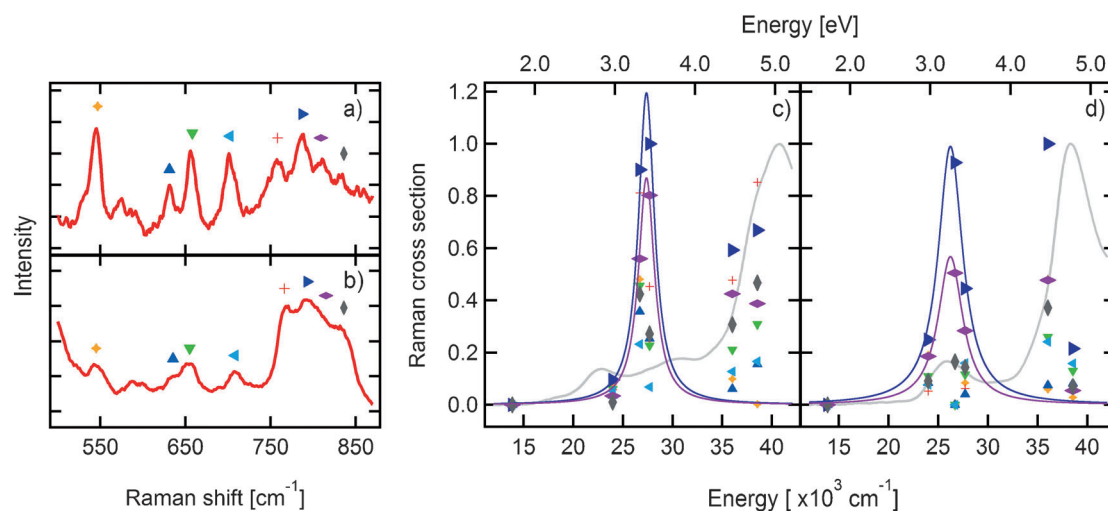


Figure 3. a) Raman spectrum of **1** in MeCN upon excitation at 2.97 eV. b) Raman spectrum of **4** in MeCN upon excitation at 4.46 eV. c) Dependence of the Raman intensity on incident photon energy for **1** in MeCN. d) Dependence of the Raman intensity on incident photon energy for **4** in MeCN. Colored symbols were used to indicate Raman peaks and their resonance behavior. The gray line denotes the absorption spectrum, whereas the colored curves serve as a guide to the eye. Incident photon energies: 1.72 eV, 2.97 eV, 3.31 eV, 3.43 eV, 4.46 eV, 4.78 eV.

putting the spectrum into a preresonance explaining the difference between the calculated with the observed spectra.

We find that selected Raman peaks of both complexes turn into resonance at 3.40 and 4.45 eV (Figure 3c,d), namely the peaks at 650, 778, and 811 cm^{-1} for **1** (Cu^{I}) and at 790 and 815 cm^{-1} for **4** (Cu^{II}). Since these vibrations are resonant at similar energies for both complexes, we relate them to vibrations, which connect the crystallographically determined structures of both oxidation states within a charge-transfer process.

Tables S3 and S4 list the geometrical changes during the vibrations for **1** and **4** together with a detailed assignment. For **1**, the vibration at 800 cm^{-1} can be related to the experimental vibration at 788 cm^{-1} (purple triangle), which is a Cu–N_{gua} stretching vibration with concomitant twist of the two chelate planes relative to each other. Precisely these two structural changes are the most important distortions between Cu^{I} and Cu^{II} geometry. For **4**, the peak at 815 cm^{-1} is assigned as a Cu–N_{gua} stretching vibration as well. Analysis of the excited singlet states attained by resonant excitation at 3.4 eV shows that for Cu^{I} the twist angle diminishes by 7° and the Cu–N_{gua} bond contracts by 0.07 Å (Figure 4c, **1^{ex}**). In the reverse sense, the excited state of the Cu^{II} complex (**4^{ex}**) displays an increase in the twist angle of 21° and a Cu–N_{gua} bond elongation of 0.1 Å.

DFT analysis^[30] of the optical transition at 3.4 eV of the Cu^{I} complex reveals that this is a metal-to-ligand charge transfer (MLCT, electron density difference map in Figure 4d). The corresponding transition of the copper(II) complex is a LMCT which is complementary to the MLCT of Cu^{I} (Figure 4e). Hence, we have successfully identified the vibronic mode that connects Cu^{I} and Cu^{II} .

Resonance Raman spectroscopy probes the electronic states that are most relevant for the vibrational excitation spectrum. In particular, a vibrational excitation mediating charge transfer will become resonant very close to the energy

of the involved electronic charge-transfer transition that connects the involved electronic orbitals.^[31,32] This resonance is expected to be much sharper and better defined in energy than UV/Vis absorptions since the resonance Raman signals are only related to one specific contribution of the charge transfer selected by the specific vibration and by doing so this technique effectively probes the reaction coordinate. Thus, the LMCT and MLCT identified by Raman spectroscopy occur in close proximity to each other as they access the inverse reaction coordinate through complementary charge-transfer processes.

In summary, we present five complexes with very similar coordination midway between tetrahedral and square-planar geometry: The oxidation of Cu^{I} to Cu^{II} increases the twist angle formed by the CuN_2 planes by only 20°. The two complex types are connected through a reversible electron transfer. X-ray absorption spectroscopy not only verifies the oxidation states of the reported complexes; it is also in excellent agreement with crystallographic data and demonstrates that the structures are independent of the complexes being solid or in solution. Moreover, the structures are independent of the choice of counterions which is supported by Raman spectroscopy. Hence, the coordination geometry is not a result of solid-state effects but inherent to the effects resulting from the balance between electronic and steric effects. Raman spectroscopy in solution allows access to the reaction coordinate of the electron transfer. Both complex types show resonance at an incident photon energy of 3.4 eV. DFT analysis reveals that at resonance a vibrational mode of Cu–N_{gua} stretching and chelate angle torsion couples with an MLCT from Cu^{I} to Cu^{II} and an LMCT from Cu^{II} to Cu^{I} . This proves that the ET transition state is optically accessible and that the concept of ligand restrictions imposed upon copper coordination is very useful for the generation of electron-transfer models.

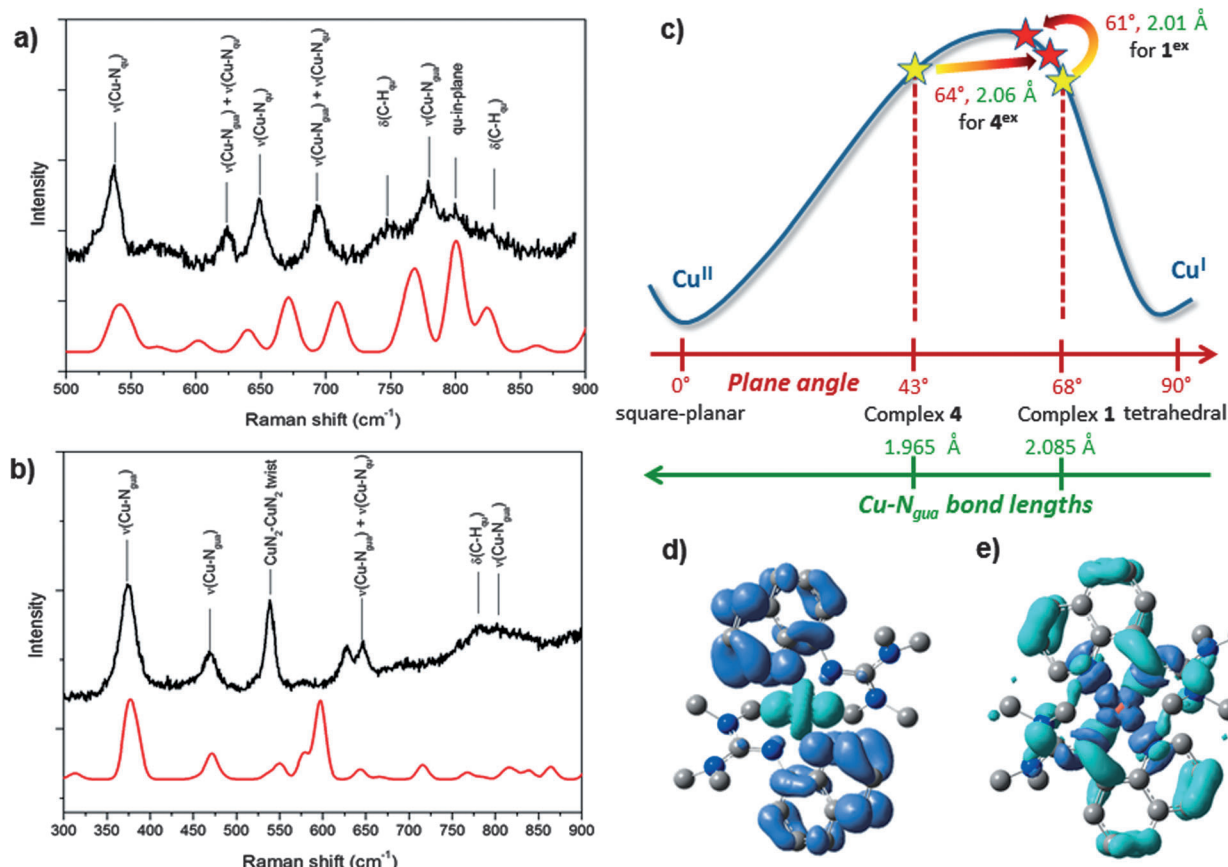


Figure 4. a) Comparison of nonresonant experimental (black) Raman spectrum at 2.97 eV and theoretical (red) Raman spectrum of **1**. b) Comparison of nonresonant experimental (black) Raman spectrum at 2.97 eV and theoretical (red) Raman spectrum of **4**. c) Reaction coordinate between Cu^I and Cu^{II} and the optically attained excited states. d) EDDM of the Cu d_{z²} → π* transition (light to dark). e) EDDM of the π → Cu d transition (light to dark)

Received: July 12, 2013

Revised: August 25, 2013

Published online: November 7, 2013

Keywords: bioinorganic chemistry · copper · resonance Raman spectroscopy · X-ray absorption spectroscopy · X-ray diffraction

- [1] E. I. Solomon, R. G. Hadt, *Coord. Chem. Rev.* **2011**, 255, 774–789.
- [2] S. G. Bratsch, *J. Phys. Chem. Ref. Data* **1989**, 18, 1–21.
- [3] A. B. P. Lever, *Inorg. Chem.* **1990**, 29, 1271–1285.
- [4] D. B. Rorabacher, *Chem. Rev.* **2004**, 104, 651–697.
- [5] P. Comba, M. Kerscher, *Coord. Chem. Rev.* **2009**, 253, 564–574.
- [6] H. B. Gray, B. G. Malmström, R. J. Williams, *J. Biol. Inorg. Chem.* **2000**, 5, 551–559.
- [7] K. M. Lancaster, S. DeBeer George, K. Yokoyama, J. H. Richards, H. B. Gray, *Nat. Chem.* **2009**, 1, 711–715.
- [8] K. M. Lancaster, O. Farver, S. Wherland, E. J. Crane III, J. H. Richards, I. Pecht, H. B. Gray, *J. Am. Chem. Soc.* **2011**, 133, 4865–4873.
- [9] K. M. Lancaster, M.-E. Zaballa, S. Sproules, M. Sundararajan, S. DeBeer, J. H. Richards, A. J. Vila, F. Neese, H. B. Gray, *J. Am. Chem. Soc.* **2012**, 134, 8241–8253.
- [10] J. J. Warren, K. M. Lancaster, J. H. Richards, H. B. Gray, *J. Inorg. Biochem.* **2012**, 115, 119–126.

- [11] B. E. Bursten, *J. Am. Chem. Soc.* **1982**, 104, 1299–1304.
- [12] B. L. Vallee, R. J. P. Williams, *Proc. Natl. Acad. Sci. USA* **1968**, 59, 498–505.
- [13] P. Comba, *Coord. Chem. Rev.* **1999**, 182, 343–371.
- [14] P. Comba, W. Schiek, *Coord. Chem. Rev.* **2003**, 238–239, 21–29.
- [15] P. Comba, V. Müller, R. Remenyi, *J. Inorg. Biochem.* **2004**, 98, 896–902.
- [16] G. Chaka, J. L. Sonnenberg, H. B. Schlegel, M. J. Heeg, G. Jaeger, T. J. Nelson, L. A. Ochrymowycz, D. B. Rorabacher, *J. Am. Chem. Soc.* **2007**, 129, 5217–5227.
- [17] a) P. Frank, M. Benfatto, R. K. Szilagy, P. D'Angelo, S. Della Longa, K. O. Hodgson, *Inorg. Chem.* **2005**, 44, 1922–1933; b) P. Frank, M. Benfatto, B. Hedman, K. O. Hodgson, *Inorg. Chem.* **2012**, 51, 2086–2096.
- [18] a) V. S. Bryantsev, M. S. Diallo, W. A. Goddard III, *J. Phys. Chem. A* **2009**, 113, 9559–9567; b) M. H. M. Olsson, U. Ryde, B. O. Roos, K. Pierloot, *J. Biol. Inorg. Chem.* **1998**, 3, 109–125; c) U. Ryde, M. H. M. Olsson, B. O. Roos, A. C. Borin, *Theor. Chem. Acc.* **2001**, 105, 452–462.
- [19] M.-E. Zaballa, L. A. Abriata, A. Donaire, A. J. Vila, *Proc. Natl. Acad. Sci. USA* **2012**, 109, 9254–9259.
- [20] E. Solomon et al. in *Electron Transfer Reactions*, (Ed.: S. Isied), ACS, Washington, DC, **1997**, chap. 19, pp. 317–330.
- [21] P. Comba, *Coord. Chem. Rev.* **2000**, 200–202, 217–245.
- [22] a) B. Xie, T. Elder, L. J. Wilson, D. M. Stanbury, *Inorg. Chem.* **1999**, 38, 12–19; b) P. Comba, M. Kerscher, A. Roodt, *Eur. J. Inorg. Chem.* **2004**, 4640–4645.

- [23] A. Hoffmann, J. Börner, U. Flörke, S. Herres-Pawlis, *Inorg. Chim. Acta* **2009**, 362, 1185–1193.
- [24] M. Pasquali, C. Floriani, G. Venturi, A. Gaetani-Manfredotti, A. Chiesi-Villa, *J. Am. Chem. Soc.* **1982**, 104, 4092–4099.
- [25] J. T. York, E. C. Brown, W. B. Tolman, *Angew. Chem.* **2005**, 117, 7923–7926; *Angew. Chem. Int. Ed.* **2005**, 44, 7745–7748.
- [26] L. Yang, D. R. Powell, R. P. Houser, *Dalton Trans.* **2007**, 955–964.
- [27] V. Raab, K. Harms, J. Sundermeyer, B. Kovacevic, Z. B. Maksic, *J. Org. Chem.* **2003**, 68, 8790–8797.
- [28] L. Kau, D. J. Spira-Solomon, J. E. Penner-Hahn, K. O. Hodgson, E. I. Solomon, *J. Am. Chem. Soc.* **1987**, 109, 6433–6442.
- [29] J. E. Hahn, R. A. Scott, K. O. Hodgson, S. Doniach, S. R. Desjardins, E. I. Solomon, *Chem. Phys. Lett.* **1982**, 88, 595–598.
- [30] A. Jesser, M. Rohrmüller, W. G. Schmidt, S. Herres-Pawlis, *J. Comp. Chem.* **2013**, DOI: 10.1002/jcc.23449.
- [31] S. Herres-Pawlis, S. Binder, A. Eich, R. Haase, B. Schulz, G. Wellenreuther, G. Henkel, M. Rübhausen, W. Meyer-Klaucke, *Chem. Eur. J.* **2009**, 15, 8678–8682.
- [32] R. G. Hadt, X. Xie, S. R. Pauleta, I. Moura, E. I. Solomon, *J. Inorg. Biochem.* **2012**, 115, 155–162.
-